

## A SIMPLE MODEL FOR THE DENSITY PROFILES OF ISOLATED DARK MATTER HALOS

ELI VISBAL<sup>1,2</sup>, ABRAHAM LOEB<sup>1</sup>, AND LARS HERNQUIST<sup>1</sup>

<sup>1</sup>Institute for Theory & Computation, Harvard University, 60 Garden Street, Cambridge, MA 02138 and  
<sup>2</sup>Jefferson Laboratory of Physics, Harvard University, Cambridge, MA 02138; evisbal@fas.harvard.edu

*Draft version June 27, 2012*

### ABSTRACT

We explore the possibility that the density profiles of elliptical galaxies and cold dark matter (CDM) halos found in cosmological simulations can be understood in terms of the same physical process, collisionless gravitational collapse. To investigate this, we study a simplified model, the collapse of a perfectly cold Plummer sphere. First, we examine an N-body simulation of this model with particles constrained to purely radial orbits. This results in a final state characterized by a profile slightly steeper than  $\rho \propto r^{-2}$  at small radii and behaving as  $\rho \propto r^{-4}$  at large radii, which can be understood in terms of simple analytic arguments. Next, we repeat our simulation without the restriction of radial orbits. This results in a shallower inner density profile, like those found in elliptical galaxies and CDM halos. We attribute this change to the radial orbit instability (ROI) and propose a form of the distribution function (DF) motivated by a physical picture of collapse. As evidence of the link between our model and CDM halos, we find that our collapse simulation has a final state with pseudo-phase-space density which scales roughly as  $\rho/\sigma^3 \propto r^{-1.875}$ , like that observed in CDM halos from cosmological simulations (Navarro et al. 2010). The velocity anisotropy profile is also qualitatively similar to that found near the centers of these halos. We argue that the discrepancy at large radii (where CDM halos scale as  $\rho \propto r^{-3}$ ) is due to the presence of the cosmological background or continued infall. This leads us to predict that the outer CDM halo density profile is not “universal,” but instead depends on cosmological environment (be it an underdense void or overdense region).

*Keywords:* Cosmology: theory — dark matter — Galaxies: elliptical and lenticular, cD

### 1. INTRODUCTION

Over roughly the past 15 years, considerable attention has been directed at the possibility that halos in cold dark matter (CDM) universes may have so-called “universal” density profiles. This idea was motivated by studies of cosmological N-body simulations which found that the spherically averaged density profiles of CDM halos could be accurately fit by the same simple function for a very large range in mass (Navarro et al. 1996). This discovery led to the popular NFW profile parameterization,

$$\rho_{\text{NFW}}(r) \propto \frac{1}{(r/r_s)(1+r/r_s)^2}, \quad (1)$$

where  $r_s$  is a characteristic length scale. There have been numerous attempts to understand the physical nature of the NFW profile and other similar parameterizations. The work has mostly focused on an origin within the cosmological context, investigating the role of large-scale structure and cosmological infall and accretion (e.g. Lithwick & Dalal 2011; Dalal et al. 2010; Subramanian et al. 2000; Zukin & Bertschinger 2010a,b). These efforts have generally failed to produce a complete physical description of the processes which lead to the halo density profiles found in simulations.

It is well known that elliptical galaxies have surface density distributions described by the de Vaucouleurs  $R^{1/4}$  law (or its generalization the Sersic law) (e.g. Trujillo et al. 2004; Graham & Guzmán 2003). A convenient analytical approximation to the deprojected  $R^{1/4}$

law is given by the Hernquist model (Hernquist 1990)

$$\rho_{\text{H}}(r) \propto \frac{1}{(r/r_s)(1+r/r_s)^3}. \quad (2)$$

The NFW and Hernquist profiles are strikingly similar, only differing asymptotically at large radii. This suggests a link between the density profiles of elliptical galaxies and CDM halos. In fact, they can be accurately fit in projection by the Sersic law or in three dimensions by a related profile, the Einasto model, which has been shown to fit CDM halos more accurately than the NFW parameterization (Merritt et al. 2005; Navarro et al. 2010). This similarity motivates the hypothesis that the same physical processes are responsible for the form of the density profiles in both CDM halos and elliptical galaxies.

This leads us to propose that the formation of CDM halos can be understood, at least in part, in terms of the physics of dissipationless gravitational collapse common to elliptical galaxies and CDM halos. We can apply this physics to better understand the density profiles observed in cosmological simulations. For example, the analytic arguments made 25 years ago by Jaffe (1987) and White (1987) imply that in the outer regions of isolated elliptical galaxies the density scales as  $\rho \propto r^{-4}$ . We suggest, that for dark matter halos, any deviation from this is due to continued accretion or because at large radii the cosmological background density dominates. Thus, to the extent that the structure of halos depends on their instantaneous accretion state or the local background density, the notion that CDM halos have “universal” density profiles is not accurate. In a  $\Lambda$ CDM universe, an isolated halo in a very low density environment will stop accret-

ing relatively early, and hence will achieve the limiting form  $\rho \propto r^{-4}$ . This is consistent with the results of the cosmological simulations of Dubinski & Carlberg (1991), where vacuum boundary conditions led to an outer profile with  $\rho \propto r^{-4}$ . We also note that the recent work of Lithwick & Dalal (2011) and Vogelsberger et al. (2011) demonstrates that for scale-free models, the inner halo profile is sensitive to the shape of the collapsing perturbation. This suggests that the inner profile of halos could be sensitive to environment as well.

In this paper, the first in a series of two, we explore the physics of dissipationless gravitational collapse and how it applies to the formation of CDM halos. We accomplish this with numerical experiments and analytic arguments based on a simple toy-model, the collapse of a perfectly cold (zero initial kinetic energy) Plummer sphere. In Paper 2 (in preparation) we will study the impact of cosmological effects, such as continued accretion. This will include analyzing cosmological N-body simulations to study the expected systematic dependence of the detailed profile on cosmological environment, be it an underdense void or an overdense region.

We begin the study of our collapsing Plummer sphere by performing a simulation of purely radial collapse in which non-radial motions are suppressed. This results in a final equilibrium state with a density profile slightly steeper than  $\rho \propto r^{-2}$  near the center and  $\rho \propto r^{-4}$  at large radii. However, a system composed entirely of particles on purely radial orbits will be dynamically unstable once non-radial motions are allowed, owing to the radial orbit instability (ROI), an effect first noted by Barnes et al. (1986) and Merritt & Aguilar (1985). When we remove the restriction of purely radial orbits we find a final state with a shallower inner profile more similar to that found in elliptical galaxies and CDM halos. The possibility that the ROI could play a role in structuring CDM halos has been emphasized already by Bellovary et al. (2008). Below, we examine this idea in greater depth by postulating a physically motivated form for the distribution function (DF) of systems which have relaxed through the ROI. As evidence of the link between our simple collapse model and CDM halos, we find that the final state has a pseudo-phase-space density  $\rho(r)/\sigma(r)^3 \propto r^{-1.875}$ , as observed in halos in N-body cosmological simulations (Navarro et al. 2010) and derived in self-similar secondary infall models (Bertschinger 1985).

This paper is structured as follows. In Section 2 we present the simulation of our toy-model of gravitational collapse with particles restricted to purely radial orbits. In the following section, we discuss the outer density profile of this numerical experiment and how it relates to CDM halos and elliptical galaxies. We consider the inner density profile in Section 4. Here we re-simulate the collapse from Section 2 without the restriction of purely radial orbits, and discuss the impact of the ROI. In Section 5 we propose a physically motivated DF for the final state of systems formed through initially radial gravitational collapse. We discuss our results in the context of previous work in Section 6 and give our main conclusions in Section 7.

Throughout the paper, the data from our numerical experiments are presented in the internal units we use in the GADGET N-body code (Springel 2005). Distances

are given in units of 1kpc, velocities in units of  $1\text{km s}^{-1}$ , and mass in units of  $10^{10}M_{\odot}$ . Other units (e.g. time, energy, density) are given by the relevant combination of these three quantities.

## 2. A SIMPLE EXAMPLE

We begin the exploration of our simplified model with an N-body simulation of gravitational collapse where particle orbits are constrained to be completely radial. The simulation was initialized as a perfectly cold (all particles with zero velocity) Plummer sphere with scale length of 100 and total mass of 100 in the code units described above. These choices are unimportant, as neither the total mass nor the scale length affect the shape of the density profile for the final state. The system was evolved in time with particles only subjected to the component of the gravitational force in the radial direction. This was accomplished by modifying the publicly available N-body code GADGET (Springel 2005). The simulation was run until it reached an equilibrium state, with the density profile plotted in Figure 1. We have achieved convergence in the sense that the final state is not sensitive to the number of particles included in the simulation. For the results shown, we used  $10^5$  particles which were initially distributed by randomly drawing from a probability density function (PDF) proportional to the Plummer profile. A gravitational softening length of  $\epsilon_g = 0.3$  was adopted; reducing this value did not affect the results on the scales of interest. Note that the specific choice of a Plummer sphere does not have a strong impact on the final state. We find similar outcomes with other initial density profiles (e.g. Gaussian or Hernquist).

Our simulation results in an equilibrium state slightly steeper than  $\rho \propto r^{-2}$  at small radii and  $\rho \propto r^{-4}$  at large radii. We can show that in general, a density profile formed through purely radial collapse cannot be shallower than  $\rho \propto r^{-2}$  using fairly simple analytical arguments (Dalal et al. 2010). In the central regions, the time averaged contribution to the total density profile from each particle is

$$\rho_p(r) \propto \frac{dt(r)}{4\pi r^2 dr} \propto \frac{1}{r^2} \frac{dt}{dr}, \quad (3)$$

where  $dt(r)$  is the time the particle spends between radii  $r$  and  $r+dr$ . For a density profile shallower than  $\rho \propto r^{-2}$ ,  $dt/dr$  is a constant for sufficiently small  $r$ . It follows from equation (3) that central density profiles must always be at least as steep as  $\rho \propto r^{-2}$  in the purely radial case.

The large radius limit can be explained with the following argument (White 1987; Jaffe 1987). In the final state of a system formed through gravitational collapse, the outer envelope will be populated by particles which have been scattered into weakly bound orbits. The size of these orbits will be inversely proportional to the energy,  $E$ . The number of particles between  $E$  and  $E+dE$ ,  $N(E)dE$ , is expected to be non-zero and continuous near  $E = 0$ . For the density, this implies

$$\rho(r) = \frac{N(E)}{4\pi r^2} \frac{dE}{dr} \propto \frac{N(GM/r)}{r^2} \frac{d(GM/r)}{dr} \propto r^{-4}. \quad (4)$$

Note that this result was derived in the context of elliptical galaxies and has been completely ignored in the literature on cosmological CDM halo formation.

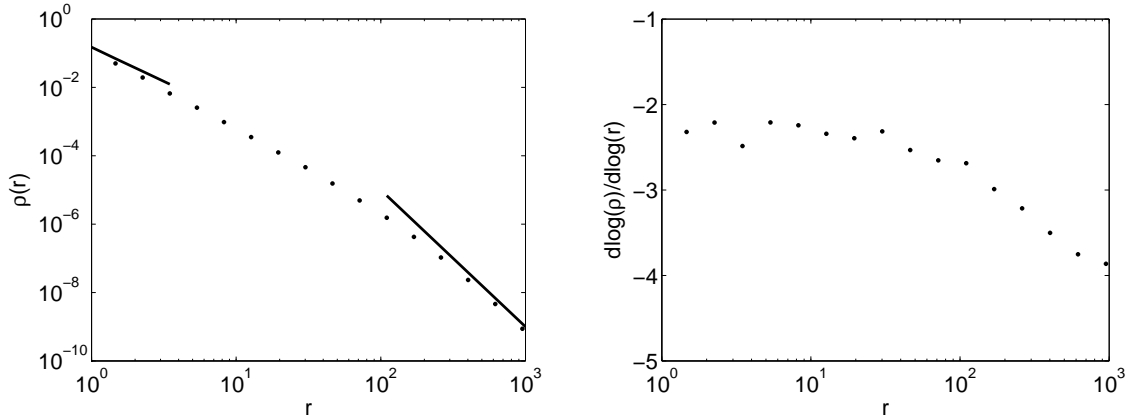


**Figure 1.** The density profile (left panel) and logarithmic slope (right panel) of the final state from our simulation of purely radial collapse starting from a perfectly cold Plummer sphere (see Section 2 for more details). The solid lines indicate  $\rho \propto r^{-2}$  at small radii and  $\rho \propto r^{-4}$  at large radii.

Although the above discussion is (intentionally) highly idealized, it demonstrates some important consequences. First, there is nothing mysterious or pathological about density profiles which diverge as  $r \rightarrow 0$ . Second, the large- $r$  behavior is consistent with the analytical arguments of White (1987) and Jaffe (1987). Note that while “violent-relaxation” (Lynden-Bell 1967) plays a role in the evolution by redistributing energy among the particles, and hence promoting a small fraction to unbound orbits, it does not in detail determine the limiting behavior at small and large radii, and hence does not justify efforts to understand the nature of the generic density profiles based on thermodynamic arguments (e.g. Spergel & Hernquist 1992). Finally, the lack of sensitivity to the number of particles indicates that the outcome has been determined by the physics of collisionless dynamics. We argue that the physical processes acting in this example are, at least in part, responsible for the origin of the density profiles of dark matter halos. While the density profile obtained from this example does not match the NFW form, we can nevertheless use it as a starting point for the more detailed study described in the following sections.

Before moving on, we note that the final state in this example can be approximated by the density profile of the Jaffe model,

$$\rho_J(r) \propto \frac{1}{(r/r_s)^2 (1 + r/r_s)^2}. \quad (5)$$

However unlike the isotropic Jaffe model, the velocities are purely radial and therefore are dynamically unstable when particles are permitted to have non-radial velocities (as we explore below). Note that the DF for a Jaffe model density profile constrained to purely radial orbits can be expressed analytically. We derive this expression in the Appendix.

### 3. THE OUTER DENSITY PROFILE

According to the arguments put forward by White (1987) and Jaffe (1987), an isolated collisionless system evolving into equilibrium through collapse should eventually achieve the limiting form  $\rho \propto r^{-4}$  at large radii. This expected outcome is in agreement with the simple numerical experiment presented in Section 2. Note that the analytic argument is insensitive to orbital anisotropy,

and therefore is unaffected by the imposed constraint of purely radial orbits. We point out that this large radius behavior should also occur in dark matter halos once cosmological infall terminates. Dubinski & Carlberg (1991) originally demonstrated this using cosmological simulations in which they employed vacuum boundary conditions around individual objects which naturally led to a cessation of late time accretion.

We suggest that the NFW profile at large radii,  $\rho \propto r^{-3}$ , does not directly reflect the physical processes that form CDM halos. We find in our collapse simulations (both the purely radial case discussed above and the generalized case discussed below) that the density profile reaches  $\rho \propto r^{-4}$  roughly two orders of magnitude beyond the radius where  $d\ln(\rho)/d\ln(r) \approx -2$ . For most CDM halos in the cosmological context, the background density will dominate at such large radii. Thus, CDM halos may not extend far enough before falling below the background density to achieve  $\rho \propto r^{-4}$ . Additionally, continued infall in high density regions could alter the outer profile. This finding has important implications for understanding the formation of halos in a cosmological context. Low-density regions will behave as open universes, implying that accretion there will halt earlier than in higher density environments. Some regions may be underdense enough to permit halos to reach the asymptotic form  $\rho \propto r^{-4}$ . Therefore, it is expected that the outer profiles of halos may exhibit a variety of behaviors, depending on environment and redshift, so in detail the outer profiles of dark matter halos will not be characterizing by a universal form. This will be explored in detail in paper 2 (in preparation).

### 4. THE INNER DENSITY PROFILE AND THE RADIAL ORBIT INSTABILITY

To investigate the small-radii properties of equilibrium systems formed through gravitational collapse, we generalize the numerical experiment described in Section 2. We perform the same N-body simulation of radial collapse, but relax the restriction that the particles move on purely radial orbits. Here we use  $2 \times 10^6$  particles and a softening length of  $\epsilon_g = 0.1$ . We find that we have achieved convergence in the sense that increasing particle number or decreasing softening length do not impact our results on the scales of interest. Since our results are not

sensitive to particle number, we conclude that 2-body relaxation does not impact our results and the system is effectively collisionless. As in the purely radial simulation, different initial density profiles result in similar final equilibrium states. The results of this simulation are presented in Figure 2. Note that the simulation was run roughly five times the dynamical time at the maximum radius shown. While we may not have reached perfect equilibrium at this radii, we do not expect substantial changes at longer times.

Initially the system has mainly radial orbits (as in the first numerical experiment). However, in response to small non-radial perturbations, purely radial orbits are dynamically unstable. The system achieves a different equilibrium in which the orbits in the inner regions are isotropic, but those in the outer regions, where the system is not strongly self-gravitating, are still mainly radial. Roughly, the transition occurs at the half-mass radius of the new configuration. This is shown in Figure 2, where we plot the radial profile of the anisotropy parameter,

$$\beta(r) = 1 - \frac{\sigma_t(r)^2}{2\sigma_r(r)^2}, \quad (6)$$

where  $\sigma_r(r)^2$  and  $\sigma_t(r)^2$  are, respectively, the radial and the tangential variance in the velocity as a function of radius ( $\beta = 0$  corresponds to isotropic and  $\beta = 1$  to radial). In the final state, the system has an inner density profile shallower than  $r^{-2}$ , but the outer regions are unchanged compared to the purely radial case, still having  $\rho \propto r^{-4}$ . The particles in this outer region (well outside the half-mass radius) respond to the gravitational potential dictated by the inner region, and their orbits are therefore stable. The inner core (inside the half mass radius), on the other hand, is self-gravitating and subject to the ROI. The resulting central density cusp is now more similar to those which characterize CDM halos and the deprojected  $R^{1/4}$  law, supporting the notion that CDM halos and elliptical galaxies are shaped by similar processes.

As further evidence of the relationship between the physics of gravitational collapse in this example and CDM halos we observe that the pseudo-phase-space density of the final state scales roughly as  $\rho/\sigma^3 \propto r^{-1.875}$ , matching that in halos from cosmological simulations (Navarro et al. 2010). This is plotted in Figure 3. We also find that the velocity anisotropy profile scales roughly as  $\beta(r) \propto \ln(r)$  near the center, qualitatively similar to that seen in halos from cosmological N-body simulations.

## 5. A DISTRIBUTION FUNCTION FOR THE RELAXED SYSTEM

The numerical experiments and analytic arguments presented in the preceding sections have led us to propose a simple scenario for how collisionless systems are formed through gravitational collapse. The outer profile is determined by the redistribution of energy among particles through violent-relaxation, which promotes a small fraction of the mass onto unbound orbits. If no further infall occurs, the density profile will asymptote to  $\rho \propto r^{-4}$  as predicted by White (1987) and Jaffe (1987). If infall has not halted, the system will not be in equilibrium and a different density profile may be measured at large radii.

For a nearly radial infall, the ROI will operate causing the system to evolve such that the inner region is characterized by orbit isotropy and a density profile shallower than  $\rho \propto r^{-2}$  (not permitted in the purely radial case). If the collapsing particles initially have significant non-radial motions, the final profile will be even shallower.

To understand the physical nature of systems formed through this scenario, we have performed an analysis of the phase-space distribution of the final state in the numerical example of Section 4. Note that because the system is anisotropic, the DF cannot be expressed as a function of energy alone. We propose the following form of the DF (guided by Gerhard (1991)),

$$f(E, L) = f(E, x) = g(E)h(x, E), \quad (7)$$

where  $x = L/L_c(E)$  is the angular momentum divided by the angular momentum of a particle on a circular orbit with energy  $E$ . The values of  $x$  range between 0 and 1. The functions  $g$  and  $h$  are given by

$$g(E) = A \exp(-\beta_E E)(-E)^c, \quad (8)$$

and

$$h(x, E) = \exp(-x^2/q(E)^2), \quad (9)$$

where  $A$ ,  $\beta_E$ , and  $c$  are free parameters. We expect  $q(E)$  to be a function which increases with  $|E|$  and parameterize it with a broken power law as explained below.

This model's main features can be explained in terms of the collapse scenario described above. The function  $h(x, E)$  determines how anisotropic orbits of a given energy are, with a delta function in  $x$  corresponding to purely radial and a constant function corresponding to isotropic. We expect that  $q(E)$  gets larger for increasing  $|E|$  such that  $h(x, E)$  transitions from a delta function for the least tightly bound particles to a constant for the most tightly bound particles. The most tightly bound particles are those which make up the inner profile and have been isotropized through the ROI, while the more weakly bound particles are unaffected by this instability and are found mostly in the outskirts of the system on radial orbits. The energy dependence of the DF in equation (8) is a Maxwellian distribution for large  $|E|$ , but modified by the factor  $(-E)^c$  for the least tightly bound particles. We can interpret this as a Gaussian distribution (representing a favorable statistical state), modified at high energies due to particles being scattered into unbound orbits. The values of the parameters in our model can also be related to the bulk properties of the system. Our expectation is that the parameter  $1/\beta_e$  is of the order of the kinetic energy per particle. The transition in  $q(E)$  which changes  $h(x, E)$  from a delta function to a constant should happen roughly at the mean energy of particles found at the half-mass radius of the system. This corresponds to the notion that the ROI isotropizes roughly the inner half of the system and leaves the outer envelope, which is not strongly self-gravitating, mostly radial.

We compare the DF measured directly from the simulation with a parameterization of this model. Values of  $c = 0.9275$  and  $\beta_E = 4 \times 10^{-5}$  are found to match the simulation well (see Figure 4). As expected, the value of  $\beta_E$  also corresponds roughly to the reciprocal of the mean kinetic energy,  $\bar{v}^2/2 = 10^4$ . For  $q(E)$  we use a broken power law of the form  $q(E) = a(-E)^b$ .

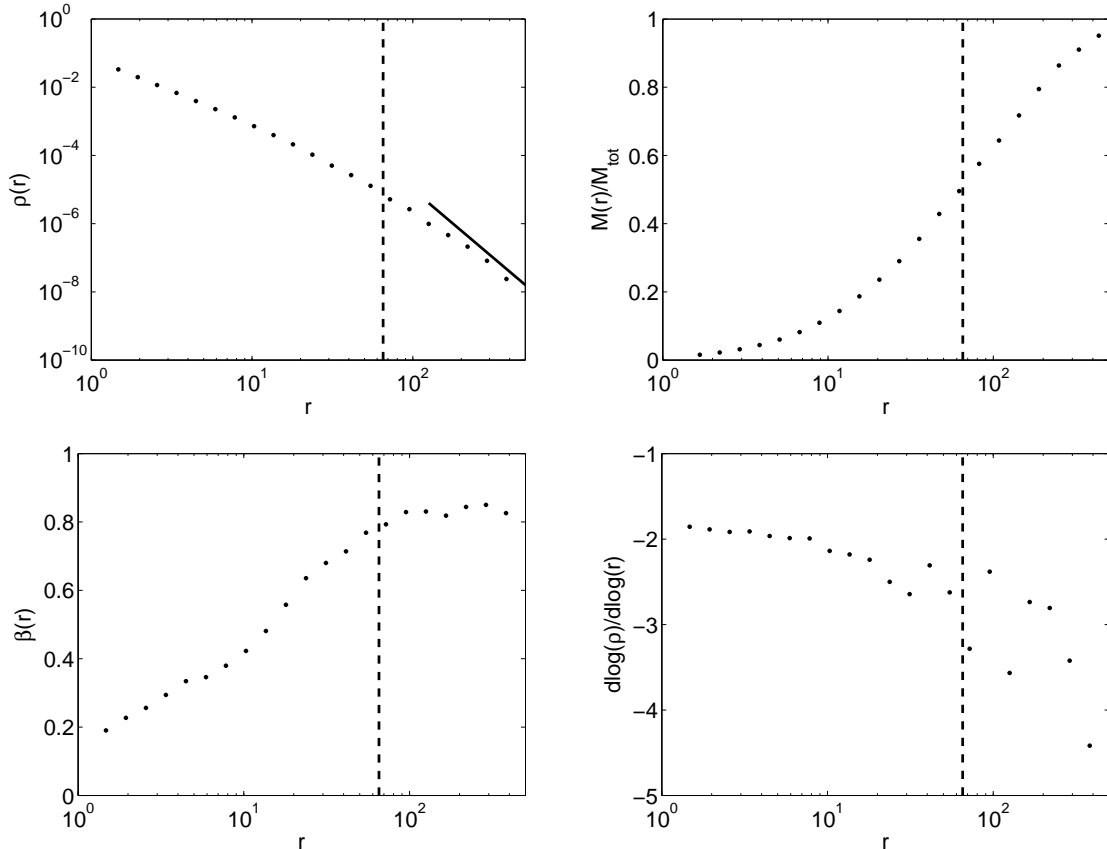


**Figure 2.** The final state of the N-body simulation of collapse from a cold (zero velocities) Plummer sphere described in Section 4. We plot radial profiles of the density (upper left), cumulative mass interior to a radius  $r$  (upper right), anisotropy parameter (lower left), and logarithmic slope (lower right). The solid line indicates  $\rho \propto r^{-4}$  and the dashed line marks the half-mass radius.

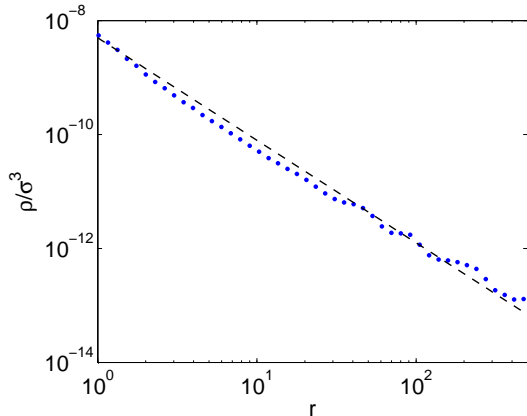


**Figure 3.** The pseudo-phase-space density,  $\rho/\sigma^3$ , of the final state of the collapse simulation described in Section 4 (points). For reference we plot  $\rho/\sigma^3 \propto r^{-1.875}$ , which is found in CDM halos from cosmological N-body simulations.

For  $\ln(-E) < 9.55$ ,  $a = 0.00012$  and  $b = 0.87$ , while for  $9.55 < \ln(-E) < 11.9$ ,  $a = 0.07$  and  $b = 0.21$ . When  $\ln(-E) > 11.9$ , we assume  $a = 4 \times 10^{-11}$  and  $b = 2$ . This was determined by fitting for  $q(E)$  separately in each energy bin and then using the power law as a simple way to parameterize the values. This procedure provides a reasonably good match to the simulation data and has the limiting behavior we expect for high and low  $E$ . We compare contours of the DF,  $f(E, L)$ , from the simula-

tion and this parameterization of the model in Figure 4. Clearly, there is very good agreement.

In addition to fitting the phase-space data from the numerical experiment we also take this DF parameterization and self-consistently compute the density and anisotropy profiles of the system. This was accomplished iteratively with the following expression:

$$\rho_{n+1}(r) = \int d^3\mathbf{v} f(E = v^2/2 + \Phi(r), L = v_t r), \quad (10)$$

where the gravitational potential  $\Phi(r)$  is computed using the density from the previous step,  $\rho_n$ . At each step the normalization of the DF is set to fix the innermost value of  $\rho(r)$  to a constant value. We use the density profile from the simulation as  $\rho(r)_1$  and iterate until the profile has converged to values where  $\rho(r)_n = \rho(r)_{n+1}$ . In Figure 5, we show the results of this procedure and find good agreement with the density and anisotropy profiles measured from the simulation. Note that we have not searched the parameter space for the best match between profiles. We simply used the same parameters described above. A better match would be obtained if we searched explicitly for the values of  $c$ ,  $\beta_E$ , and the  $q(E)$  power law parameters which minimize the density profile discrepancy. More flexible functions of  $q(E)$  could also improve the fit.

That a relatively simple form of the DF matches the results of our numerical experiments so well justifies the notion that there is favored outcome through gravitational

collapse. A similar outcome should apply to all systems formed through radial dissipationless gravitational collapse, including CDM halos and elliptical galaxies.

## 6. COMPARISON WITH PREVIOUS WORK

There has been much work attempting to understand the physical nature of the nearly universal density profiles of CDM halos found in cosmological N-body simulations. Next we summarize much of this work and explain how it relates to the present paper.

One popular way of analytically modeling CDM halo formation is through so-called secondary infall (SI) models. This work began with Gunn & Gott (1972), who studied how mass shells accrete onto a collapsed object. Later, by imposing self-similar and radial orbits Bertschinger (1985) and Fillmore & Goldreich (1984) were able to derive the inner profile of a halo as a function of the density profile of the initial perturbation. More recently, there have been a number of improvements to these models which include angular momentum (Zukin & Bertschinger 2010a,b) and generalize to fully 3D solutions (Lithwick & Dalal 2011), including numerical simulations (Vogelsberger et al. 2011). Note that much like our example in Section 2, the purely radial SI models produce halos which have steeper central profiles than those observed in cosmological simulations. Models which include non-radial velocities are able to produce NFW or Einasto-like profiles. However, they contain a number of non-physical assumptions to make the problem tractable, such as spherical symmetry or assuming that all particles in a given mass shell have the same velocity. In this paper, we argue that much of the physics which determines the density profiles of CDM halos is unrelated to cosmology. The details related to cosmological expansion and accretion included in SI modeling may obscure the important physics. Thus, our work complements the SI approach by identifying what aspects of the equilibrium state do not depend on cosmology.

Other work focusing on the cosmological context has investigated how the hierarchical assembly of halos affects the density profile. Huss et al. (1999) found that a variety of different initial conditions, including simple monolithic collapse produce similar density profiles. Wang & White (2009) find that cosmological hot dark matter (HDM) simulations produce similar profiles to CDM halos, implying that the mergers due to increased substructure in a CDM cosmology are not important to structuring density profiles. This is also supported by the simulations of Kazantzidis et al. (2006), who find that the shape of density profiles are preserved during major mergers of halos in N-body simulations, and earlier work by Hernquist (1992, 1993); Barnes & Hernquist (1996) who showed that density profiles similar to those described here arise naturally in mergers of individual galaxies. All of this work supports the idea presented in this paper, that the shape of CDM halos is due to physical principles common to collapsing systems rather than depending on the details of initial conditions or cosmology.

It has also been observed in cosmological simulations that the outer portions of CDM halo density profiles depend on the cosmological model. For example the outskirts of halos simulated with vacuum boundary conditions have profiles steeper than the NFW profile

(Dubinski & Carlberg 1991). In the future of a  $\Lambda$ CDM universe, halos are steeper than the NFW parameterization at large radius and are truncated due to the acceleration caused by dark energy (Busha et al. 2005). We note that the analytic prediction of  $\rho \propto r^{-4}$  breaks down at large radii in this case since the binding energy of particles is affected by dark energy. That the outer profile is affected by cosmology supports our claim that the  $\rho \propto r^{-3}$  asymptotic limit in the NFW profile is a consequence of the cosmological background density and continued accretion and not due to the primary physics which determines the profile.

We argue that the ROI is a key physical process which determines the shape of CDM halo density profiles. This has been proposed by a number of other authors and the ROI has been explored both within N-body simulations (Bellovary et al. 2008; MacMillan et al. 2006) and semi-analytic models (Barnes et al. 2005). We extend these studies by proposing a form of the DF motivated by a physical scenario of gravitational collapse including the ROI. A different form of the DF to describe objects formed through gravitational collapse was put forward by Trenti & Bertin (2005) and Trenti et al. (2005). This DF was determined by maximizing entropy subject to a constraint involving an integral of the angular momentum and the energy. This model generates density and velocity anisotropy profiles similar to those found in N-body simulations, but has a feature which does not match in the detailed form of  $f(E, L)$ . Another relevant paper is Merritt et al. (2005), where they point out, as we have, that elliptical galaxy and CDM halo profiles can both be fit by similar parameterizations (namely the Einasto profile or Sersic model). In this paper we have attempted to better explain this connection by studying a new form of the DF which better matches simulations.

## 7. CONCLUSIONS

The similarity between the density profiles of CDM halos and elliptical galaxies suggests that their formation can be understood in terms of the same physical processes. This leads us to propose that the features of CDM halo density profiles result, to a large extent, from the physics of gravitational collapse of collisionless systems. In this paper, the first in a series, we studied these dynamics by exploring a toy-model, the collapse of a perfectly cold Plummer sphere.

Using analytic arguments and two numerical experiments, we demonstrated that the final equilibrium state of our Plummer model collapse can be understood in fairly simple terms. In the first experiment, we ran an N-body simulation of collapse with the particles constrained to radial orbits. In the final state, we have found an inner density profile which is slightly steeper than  $\rho \propto r^{-2}$  and an outer profile which scales as  $\rho \propto r^{-4}$ . Simple analytic arguments explain these asymptotic profiles. In the second experiment, we relaxed the radial orbit constraint. Here we have found the same outer equilibrium profile, but a shallower inner profile, which we attribute to isotropization introduced by the ROI in the self-gravitating core of the halo.

We are led to a relatively simple scenario for the formation of objects through radial gravitational collapse. Initially violent-relaxation scatters some particles to unbound orbits and the remaining weakly bound particles

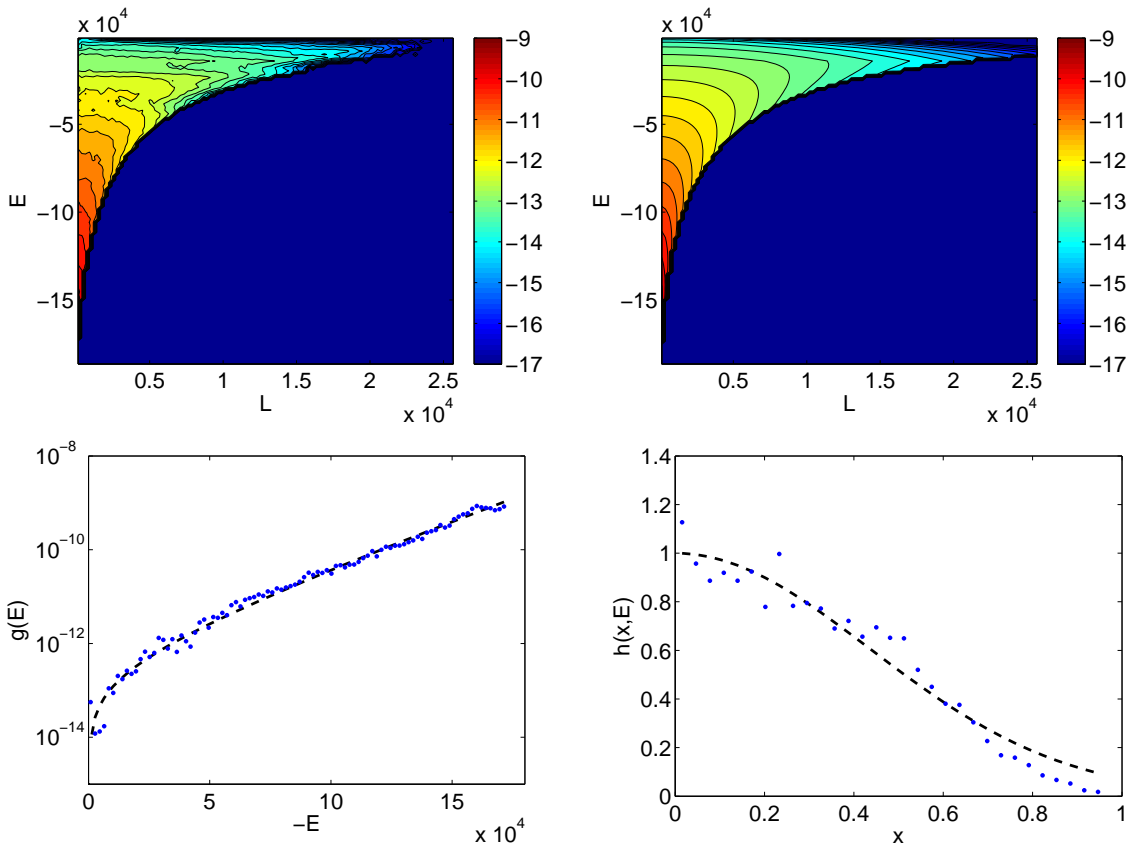


**Figure 4.** A comparison of the DF from the N-body simulation of gravitational collapse described in Section 4 and the model DF described in Section 5. We plot contours of the DF,  $\log(f(E, L))$ , from the simulation (upper left panel) and the parameterized model (upper right panel). In the lower left panel we plot  $g(E)$ , given by equation (8), for the simulation data (blue points) and the model (dashed line). In the lower right panel we plot  $h(x, E = -3.8 \times 10^4)$ , given by equation (9). The values for the model parameters are listed in the main text.

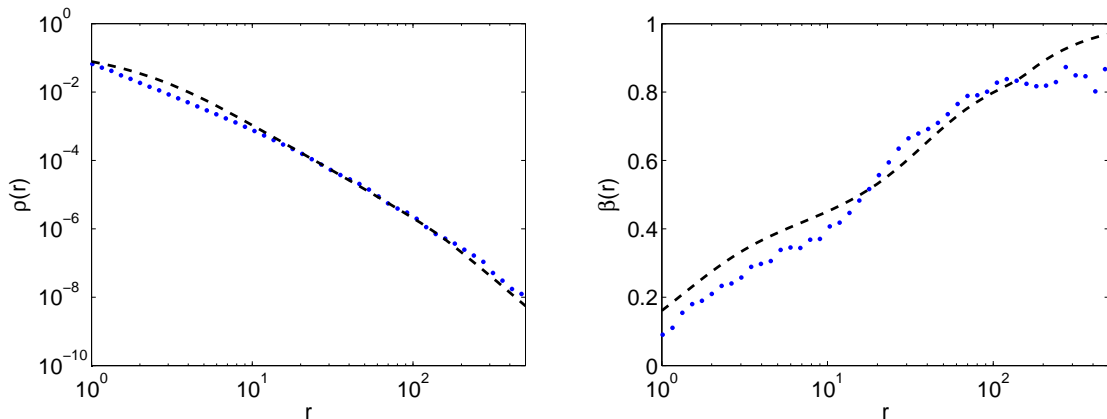


**Figure 5.** A comparison between the numerical simulation described in Section 4 and the model DF described in Section 5. We plot the density profile (left panel) and the velocity anisotropy (right panel) from the simulation (blue points) and the values implied by the model DF (dashed lines). The values for the model parameters used are listed in the main text.

form the outer density profile, which scales as  $r^{-4}$  due to the argument of Jaffe (1987) and White (1987). These particles are not strongly self-gravitating and thus remain on mostly radial orbits. The inner profile is strongly self-gravitating and becomes isotropic through the onset of ROI resulting in a profile shallower than  $\rho \propto r^{-2}$ , like those observed in elliptical galaxies and CDM halos.

We present a form of the DF which matches the final state of our collapse simulation. The main features of this model can be related to our physical picture of collapse;

weakly bound (large radii) particles are on radial orbits and tightly bound (small radii) particles have isotropic velocities. This is captured with a term that describes how circular orbits are as a function of energy,  $h(x, E)$ . These simple considerations are combined with a roughly Maxwellian energy dependence term, which is a natural expectation based on statistical arguments. Our model self-consistently reproduces the density and anisotropy profiles obtained from our simulations. The parameters in the model can also be related to the bulk properties

of the system.

The simple parameterization of the DF motivates a universal form for density profiles created through this process. However, non-radial velocities in the initial conditions of collapse may alter the inner profile, making it shallower than we find in our numerical experiments. Continued cosmological infall and accretion could also have some effect. These factors may make the inner profiles of CDM halos sensitive to cosmological parameters in detail. Since the outer profile of an object created through gravitational collapse is predicted to scale as  $\rho \propto r^{-4}$ , the shallower profile in CDM halos must be due to ongoing cosmological accretion and the presence of the cosmological background.

As evidence for the connection between our toy-model and CDM halos we find that they both have the same power law for the pseudo-phase-space density,  $\rho/\sigma^3 \propto r^{-1.875}$ . We also note that at small radii, CDM halos have an anisotropy profile,  $\beta(r)$ , which is similar to our collapse model (Navarro et al. 2010).

The physical picture presented in this paper provides

predictions for CDM halos which can readily be tested. First, there is no “universal” form of the CDM halos in the Universe. Instead, the outer halo is altered by accretion and therefore will depend on background density. In principle, a halo in a sufficiently under-dense region will behave as if it is in an open-universe, causing accretion to halt at earlier epochs allowing the halo to equilibrate to the  $\rho \propto r^{-4}$  form. Another prediction is that the final state of halos may have DFs which resemble those from our collapse simulation. We will test these predictions in paper 2 (in preparation) and further investigate how the physics of dissipationless collapse and effects from the cosmological environment combine to produce the CDM halo density profiles seen in N-body simulations.

## 8. ACKNOWLEDGMENTS

We thank Mark Vogelsberger for useful conversations. This work was supported in part by NSF grant AST-0907890 and NASA grants NNX08AL43G and NNA09DB30A.

## APPENDIX

### DISTRIBUTION FUNCTION OF THE RADIAL JAFFE PROFILE

The distribution function (DF) for a system of purely radial orbits can be written as

$$f(\mathbf{x}, \mathbf{v}) = g(\mathcal{E})\delta^D(L^2), \quad (\text{A1})$$

where  $\mathcal{E} \equiv -E$  and  $\delta^D$  is a Dirac delta function. We derive  $g(\mathcal{E})$  for a Jaffe density profile with scale length  $a$  and density parameter  $\rho_0$ ,

$$\rho(r) = \frac{\rho_0}{(r/a)^2(1+r/a)^2}. \quad (\text{A2})$$

We begin with

$$\rho(r) = \int d^3\mathbf{v} f(\mathbf{x}, \mathbf{v}) = \int dv_r \frac{g(\mathcal{E})}{r^2}, \quad (\text{A3})$$

where  $v_r$  is the radial velocity. We then perform a change of variables to obtain

$$\tilde{\rho}(r) = \int_0^\Psi \frac{d\mathcal{E}g(\mathcal{E})}{\sqrt{\Psi - \mathcal{E}}}, \quad (\text{A4})$$

where we have defined  $\tilde{\rho}(r) \equiv \sqrt{2}\rho(r)r^2$  and  $\Psi \equiv -\Phi$ . Using the Abel integral equation (see Appendix B in Binney & Tremaine (2008)), we can solve for  $g(\mathcal{E})$ ,

$$g(\mathcal{E}) = \frac{1}{\pi} \left[ \int_0^\mathcal{E} \frac{d\Psi}{\sqrt{\mathcal{E} - \Psi}} \frac{d\tilde{\rho}}{d\Psi} + \frac{\tilde{\rho}(\Psi = 0)}{\sqrt{\mathcal{E}}} \right]. \quad (\text{A5})$$

Since  $\Psi$  is a monotonic function of  $r$  we are able to use  $\tilde{\rho}$  as a function of  $\Psi$ ,

$$\tilde{\rho}(\Psi) = \sqrt{2}\rho_0 a^2 e^{-2\tilde{\Psi}} \left( e^{\tilde{\Psi}} - 1 \right)^2, \quad (\text{A6})$$

where  $\tilde{\Psi} = \Psi/(4\pi\rho_0 a^2 G)$ . Evaluating the integral in equation (A5) we obtain,

$$g(\mathcal{E}) = \frac{2a}{\pi^{3/2}} \sqrt{\frac{\rho_0}{G}} \left[ \sqrt{2}D \left( \sqrt{\frac{\mathcal{E}}{4\pi a^2 \rho_0 G}} \right) - D \left( \sqrt{\frac{\mathcal{E}}{2\pi a^2 \rho_0 G}} \right) \right], \quad (\text{A7})$$

where  $D(x)$  is the Dawson function.

## REFERENCES

Barnes, E. I., Williams, L. L. R., Babul, A., & Dalcanton, J. J. 2005, *ApJ*, 634, 775

- Barnes, J., Hut, P., & Goodman, J. 1986, *ApJ*, 300, 112
- Barnes, J. E., & Hernquist, L. 1996, *ApJ*, 471, 115
- Bellovary, J. M., Dalcanton, J. J., Babul, A., et al. 2008, *ApJ*, 685, 739
- Bertschinger, E. 1985, *ApJS*, 58, 39
- Binney, J., & Tremaine, S. 2008, *Galactic Dynamics: Second Edition* (Princeton University Press)
- Busha, M. T., Evrard, A. E., Adams, F. C., & Wechsler, R. H. 2005, *MNRAS*, 363, L11
- Dalal, N., Lithwick, Y., & Kuhlen, M. 2010, *ArXiv e-prints*
- Dubinski, J., & Carlberg, R. G. 1991, *ApJ*, 378, 496
- Fillmore, J. A., & Goldreich, P. 1984, *ApJ*, 281, 1
- Gerhard, O. E. 1991, *MNRAS*, 250, 812
- Graham, A. W., & Guzmán, R. 2003, *The Astronomical Journal*, 125, 2936
- Gunn, J. E., & Gott, III, J. R. 1972, *ApJ*, 176, 1
- Hernquist, L. 1990, *ApJ*, 356, 359
- . 1992, *ApJ*, 400, 460
- . 1993, *ApJ*, 409, 548
- Huss, A., Jain, B., & Steinmetz, M. 1999, *ApJ*, 517, 64
- Jaffe, W. 1987, in *IAU Symposium, Vol. 127, Structure and Dynamics of Elliptical Galaxies*, ed. P. T. de Zeeuw & S. D. Tremaine, 511
- Kazantzidis, S., Zentner, A. R., & Kravtsov, A. V. 2006, *ApJ*, 641, 647
- Lithwick, Y., & Dalal, N. 2011, *ApJ*, 734, 100
- Lynden-Bell, D. 1967, *MNRAS*, 136, 101
- MacMillan, J. D., Widrow, L. M., & Henriksen, R. N. 2006, *ApJ*, 653, 43
- Merritt, D., & Aguilar, L. A. 1985, *MNRAS*, 217, 787
- Merritt, D., Navarro, J. F., Ludlow, A., & Jenkins, A. 2005, *ApJ*, 624, L85
- Navarro, J. F., Frenk, C. S., & White, S. D. M. 1996, *ApJ*, 462, 563
- Navarro, J. F., Ludlow, A., Springel, V., et al. 2010, *MNRAS*, 402, 21
- Spergel, D. N., & Hernquist, L. 1992, *The Astrophysical Journal Letters*, 397, L75
- Springel, V. 2005, *MNRAS*, 364, 1105
- Subramanian, K., Cen, R., & Ostriker, J. P. 2000, *ApJ*, 538, 528
- Trenti, M., & Bertin, G. 2005, *A&A*, 429, 161
- Trenti, M., Bertin, G., & van Albada, T. S. 2005, *A&A*, 433, 57
- Trujillo, I., Erwin, P., Asensio Ramos, A., & Graham, A. W. 2004, *The Astronomical Journal*, 127, 1917
- Vogelsberger, M., Mohayaee, R., & White, S. D. M. 2011, *MNRAS*, 414, 3044
- Wang, J., & White, S. D. M. 2009, *MNRAS*, 396, 709
- White, S. D. M. 1987, in *IAU Symposium, Vol. 127, Structure and Dynamics of Elliptical Galaxies*, ed. P. T. de Zeeuw & S. D. Tremaine, 339–349
- Zukin, P., & Bertschinger, E. 2010a, *Phys. Rev. D*, 82, 104044
- . 2010b, *Phys. Rev. D*, 82, 104045